

# Supporting Information

## Construction of pillar[4]arene[1]quinone/1,10-dibromodecane pseudorotaxanes in solution and the solid state

Xinru Sheng<sup>†1</sup>, Errui Li<sup>†1</sup> and Feihe Huang<sup>\*1,2</sup>

*<sup>1</sup>State Key Laboratory of Chemical Engineering, Center for Chemistry of High-Performance & Novel Materials, Department of Chemistry, Zhejiang University, Hangzhou 310027, P. R. China; Email: [fhuang@zju.edu.cn](mailto:fhuang@zju.edu.cn)*

*<sup>2</sup>Green Catalysis Center and College of Chemistry, Zhengzhou University, Zhengzhou 450001, P. R. China*

### Table of Content (10 pages)

1.	Materials and methods	S2
2.	Characterizations of <b>H</b> and <b>G</b>	S3
3.	Crystallographic data of the [3]pseudorotaxane between <b>H</b> and <b>G</b> in the solid state	S4
4.	Characterization studies on the complexation between <b>H</b> and <b>G</b> in solution	S5
5.	References	S10

## 1. Materials and methods

All reagents and solvents were commercially available and used as supplied without further purification. **H** was synthesized according to literature procedures.<sup>S1</sup> <sup>1</sup>H NMR spectra were recorded on a temperature-controlled 400MHz, 500MHz or 600MHz spectrometer with use of the deuterated solvent as the lock and the residual solvent or TMS as the internal reference. Matrix-assisted Laser Desorption/Ionization Time of Flight Mass Spectrometry (MALDI-TOF MS) was recorded on a Bruker Ultraflex with a 355 nm Nd: YAG laser (Smartbeam II) and 25 kV Ion source voltage. UV-vis spectra were taken on a Perkin-Elmer Lambda 35 UV-vis spectrophotometer.

## 2. Characterizations of H and G

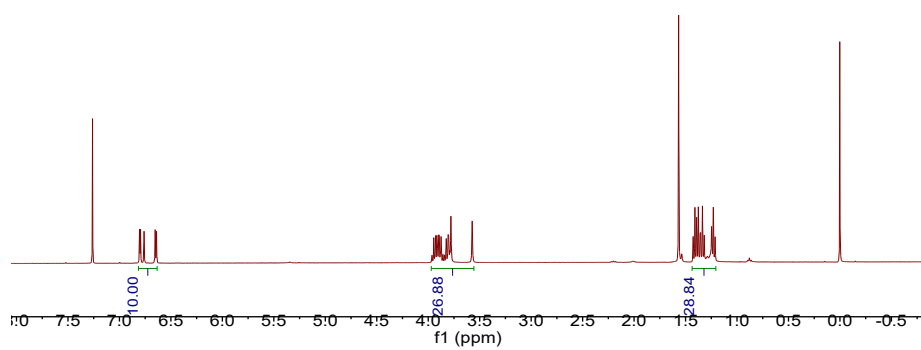


**Figure S1:** <sup>1</sup>H NMR spectrum (400 MHz, CDCl<sub>3</sub>, 298 K) of **H**.

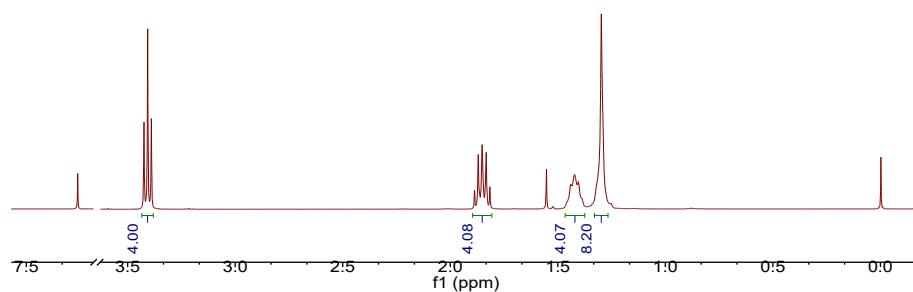


**Figure S2:** <sup>1</sup>H NMR spectrum (400 MHz, CDCl<sub>3</sub>, 298 K) of **G**.

### MALDI-TOF Mass Spectrum

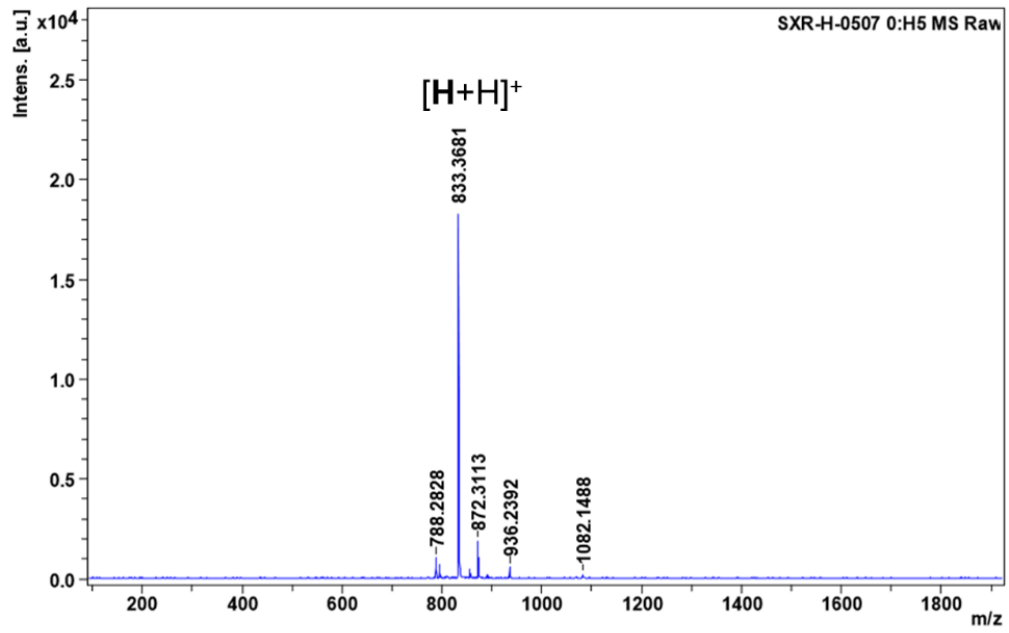


**Figure S3:** MALDI-TOF mass spectrum of **H**.

### 3. Crystallographic data of the [3]pseudorotaxane between H and G in the solid state

**Table S1. Crystal data for single crystals of the [3]pseudorotaxane between H and G in the solid state**

Empirical formula	$C_{112}H_{140}Br_2O_{20}$
Formula weight	1966.06
Temperature	170 K
Wavelength	0.71073
Crystal system	Monoclinic
Space group	$P 1 2_1/c 1$
Unit cell dimensions	$a = 17.4426(6) \text{ \AA}$ $\alpha = 90$ $b = 19.3528(8) \text{ \AA}$ $\beta = 96.800(1)$ $c = 15.3931(4) \text{ \AA}$ $\gamma = 90$
Volume	5159.6(3)
Z	4
Density (calculated)	1.265 g/cm <sup>3</sup>
Absorption coefficient	0.854
F(000)	2084.0
Crystal size	0.336 x 0.139 x 0.116 mm <sup>3</sup>
Theta range for data collection	2.35 to 27.40°
Index ranges	-19 ≤ h ≤ 22, -25 ≤ k ≤ 20, -19 ≤ l ≤ 19
Reflections collected	41520
Independent reflections	11778 [R(int) = 0.0705]
Completeness to theta = 27.492°	0.996
Absorption correction	Multi-scan
Max. and min. transmission	0.746, 0.686
Data / restraints / parameters	11778 / 0 / 612
Goodness-of-fit on F <sup>2</sup>	1.046
Final R indices [I > 2σ(I)]	R1 = 0.0480, wR2 = 0.0511
R indices (all data)	R1 = 0.0705, wR2 = 0.0672
Largest diff. peak and hole	0.561, -0.709 e. Å <sup>-3</sup>
CCDC	2031286

#### 4. Characterization studies on the complexation between **H** and **G** in solution

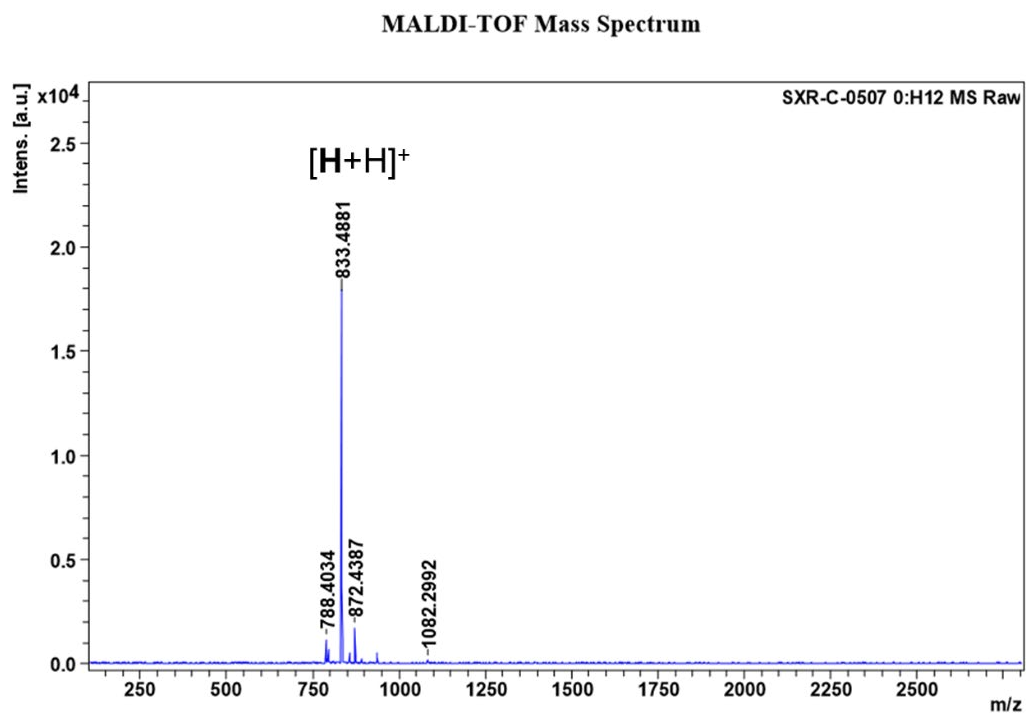


**Figure S4:** MALDI-TOF mass spectrum of **H** and **G**. There only exist the peaks of **H**.

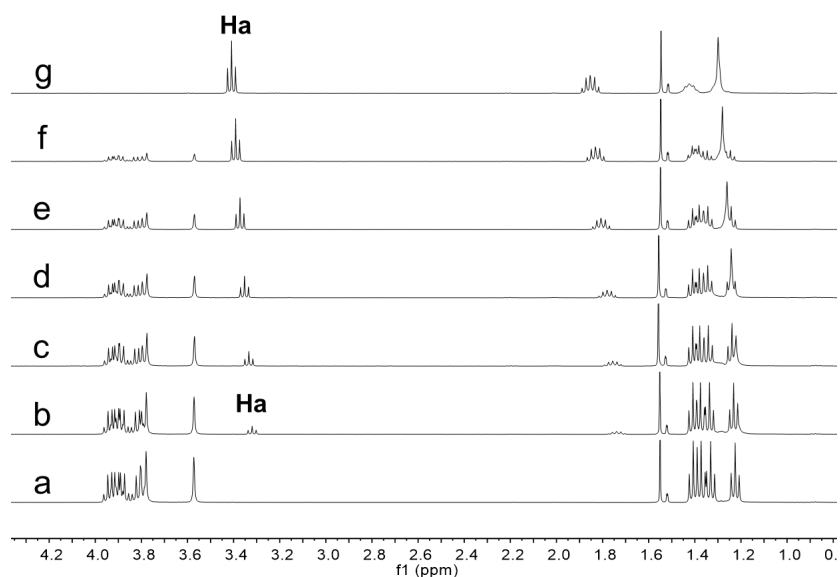


**Figure S5:** Partial  $^1\text{H}$  NMR spectra (500 MHz, chloroform-*d*, 298 K): (a) 6.00 mM **H**; (b) 1.00 mM **G** and 5.00 mM **H**; (c) 2.00 mM **G** and 4.00 mM **H**; (d) 3.00 mM **G** and 3.00 mM **H**; (e) 4.00 mM **G** and 2.00 mM **H**; (f) 5.00 mM **G** and 1.00 mM **H**; (g) 6.00 mM **G**.

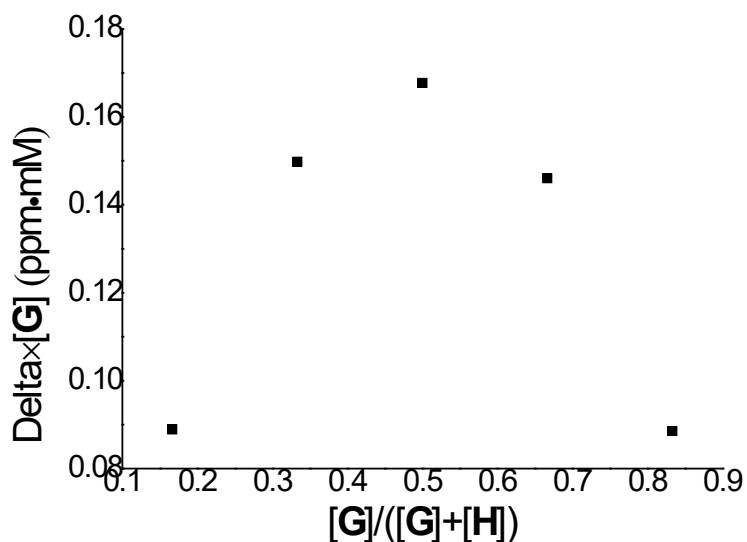


**Figure S6:** Job plot showing the 1:1 stoichiometry of the complexation between **H** and **G** in chloroform-*d* using the proton NMR data for  $\text{H}_a$ . Delta is the chemical shift change of  $\text{H}_a$ .  $[\text{H}] + [\text{G}] = 6.00$  mM.  $[\text{H}]$  and  $[\text{G}]$  are concentrations of **H** and **G**, respectively.

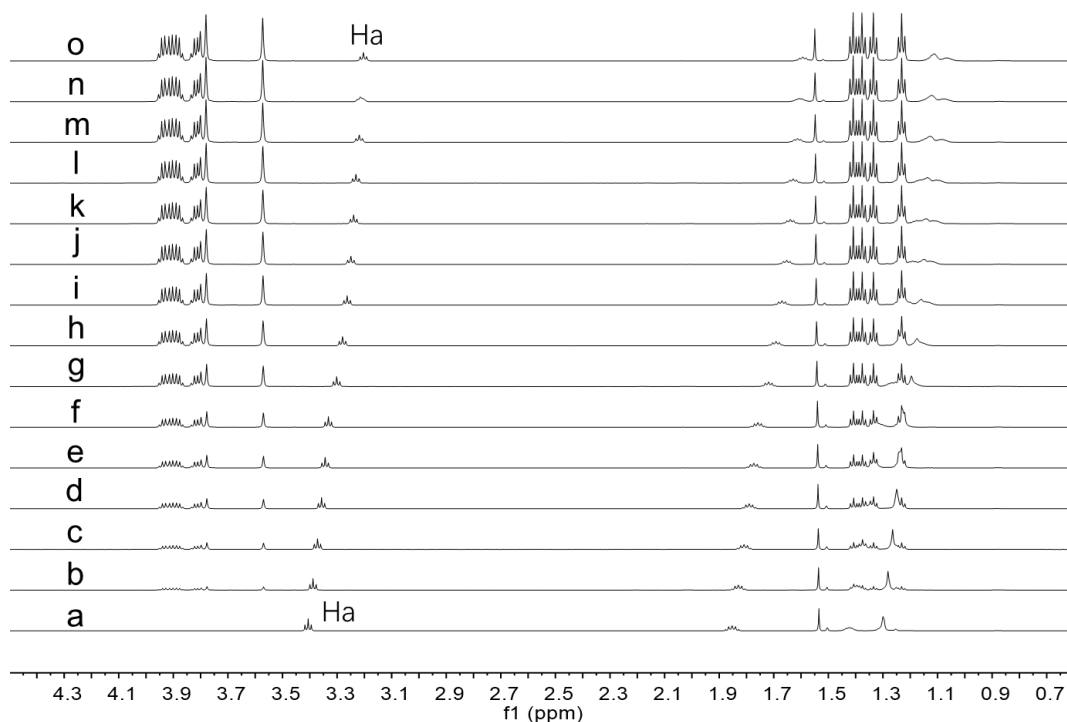


**Figure S7:** Partial  $^1\text{H}$  NMR spectra (600 MHz, chloroform- $d$ , 298 K) of **G** at the concentration of 5.00 mM upon addition of **H**: (a) 0 mM; (b) 1.16 mM; (c) 2.20 mM; (d) 3.14 mM; (e) 3.98 mM; (f) 4.74 mM; (g) 6.85 mM; (h) 8.47 mM; (i) 9.74 mM; (j) 10.77 mM; (k) 11.63 mM; (l) 12.34 mM; (m) 13.47 mM; (n) 14.33 mM; (o) 15.00 mM.

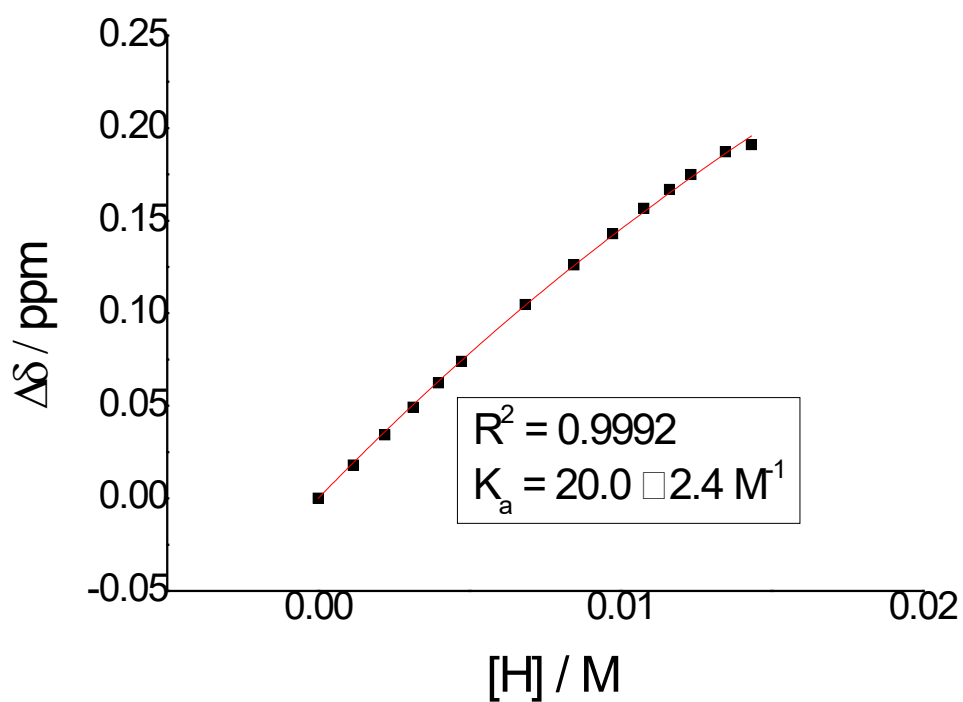


**Figure S8:** The chemical shift changes upon addition of **H**. The red solid line was obtained from the non-linear curve-fitting equation,<sup>S2</sup>  $y = (P1/[G]) (0.5x + 0.5 ([G] + P2) - (0.5(x^2 + (2x(P2 - [G])) + (P2 + [G])^2)^{0.5}))$ , where  $y = \Delta\delta$ ,  $P1 = \Delta\delta_{\text{max}}$ ,  $P2 = 1/K_a$ , and  $x = [\text{H}]$ .

## 5. References

- S1. Han, C.; Zhang, Z.; Yu, G.; Huang, F. *Chem. Commun.*, **2012**, *48*, 9876–9878.
- S2. Zhu, X.-Z.; Chen, C.-F. *J. Org. Chem.*, **2005**, *70*, 917–924.